

Optical Engineering

OpticalEngineering.SPIEDigitalLibrary.org

Development of high-resolution active matrix spatial light modulator

Yong-Hae Kim
Chi-Young Hwang
Ji Hun Choi
Jae-Eun Pi
Jong-Heon Yang
Seong-M. Cho
Sang-Hoon Cheon
Gi Heon Kim
Kyunghee Choi
Hee-Ok Kim
Won-Jae Lee
Han-Byeol Kang
Chi-Sun Hwang

SPIE.

Yong-Hae Kim, Chi-Young Hwang, Ji Hun Choi, Jae-Eun Pi, Jong-Heon Yang, Seong-M. Cho, Sang-Hoon Cheon, Gi Heon Kim, Kyunghee Choi, Hee-Ok Kim, Won-Jae Lee, Han-Byeol Kang, Chi-Sun Hwang, "Development of high-resolution active matrix spatial light modulator," *Opt. Eng.* **57**(6), 061606 (2018), doi: 10.1117/1.OE.57.6.061606.

Development of high-resolution active matrix spatial light modulator

Yong-Hae Kim, Chi-Young Hwang, Ji Hun Choi, Jae-Eun Pi, Jong-Heon Yang, Seong-M. Cho, Sang-Hoon Cheon, Gi Heon Kim, Kyunghee Choi, Hee-Ok Kim, Won-Jae Lee, Han-Byeol Kang, and Chi-Sun Hwang*

Electronics and Telecommunications Research Institute, Daejeon, Republic of Korea

Abstract. We developed a high-resolution active matrix spatial light modulator on a glass substrate. To integrate a switching device on the glass substrate, we designed a high-performance oxide thin-film transistor with a minimum channel length of 1 μm and a maximum processing temperature of 380°C. To drive a large number of data lines, we used multiple source drivers and data drivers as well. For an optical modulation, we optimized a liquid crystal of a high anisotropic refractive index of 0.25 with a cell gap of 2.5 μm , which was effectively operated until pixel pitch is 1.6 μm . Hologram was successfully reconstructed by fabricated SLM with 7- μm pixel pitch. For the other approach for a high-resolution spatial light modulator, we tested a phase change material of $\text{Ge}_2\text{Sb}_2\text{Te}_5$ [GST]. The variation of refractive index between a polycrystalline phase and an amorphous phase of the GST film is used for a hologram reconstruction. By optimizing the underlying oxide thickness, we can show a color hologram without color filters. © 2018 Society of Photo-Optical Instrumentation Engineers (SPIE) [DOI: [10.1117/1.OE.57.6.061606](https://doi.org/10.1117/1.OE.57.6.061606)]

Keywords: diffraction; hologram; spatial light modulator; oxide thin-film transistor; liquid crystal; phase change material.

Paper 171734SS received Oct. 31, 2017; accepted for publication Jan. 31, 2018; published online Feb. 26, 2018.

1 Introduction

Nowadays many people have the chance to experience three-dimensional (3-D) viewing through virtual reality devices, such as a Samsung Gear VR™ or an Oculus Rift™. Although it immerses viewers in an incredibly vivid landscape, it sometimes makes our eyes feel uncomfortable. The reason for this kind of eye fatigue is known as vergence-accommodation conflict. Light waves from the most 3-D displays do not reproduce original light waves but only imitate them for two eyes separately. However, holograms can reproduce the exact original light wave completely.¹

Analog holograms that use nanometer-sized photosensitive particles can reconstruct vivid 3-D images.² Digital holograms that use a micrometer-sized pixelated structure can also generate realistic 3-D scenes.^{3–7} Tsuchiyama and Matsushima³ were successful in making a color digital hologram using a chrome mask with a pixel pitch of 0.8 μm . They used an optimized color filter structure and LED lighting to generate a realistic color image. Williams et al.⁴ used two sets of Ag optical antennas with a pixel pitch of 0.325 μm . By changing the polarization direction of the incoming light wave with a liquid crystal, they could produce two different images from one hologram panel. Wan et al.^{5,6} used an Al nano slit structure with a pixel pitch of 0.23 μm . By changing the slit direction and the slit width, they achieved complex modulation of light waves. They could successfully produce a color hologram by adjusting the impinging direction of red, green, and blue laser lights. Malek et al.⁷ applied a gold nano rod with a pixel pitch of 0.34 μm on a stretchable substrate. By stretching the substrate, the reconstructed image was also moved.

Although digital hologram technology has been developed rapidly, active matrix spatial light modulator (AMSLM) technology, which can change a reconstructed hologram image dynamically, lags behind. Many researchers are focusing on how to downsize the display technology to micrometer size using a liquid crystal as an optical modulator.^{8–10} Holoeye⁸ recently has started to sell GAEA-2™ SLM with a pixel pitch of 3.74 μm . Because they used a liquid crystal on silicon (LCoS) technology, they can obtain a high-resolution AMSLM, but it contrarily restricted the panel size to 0.7-in. diagonal. Lee et al.⁹ reported a high-resolution AMSLM with a pixel pitch of 3.76 μm . They used a low-temperature polysilicon thin-film transistor (TFT) as a switching device on a glass substrate so that a panel size could be increased to 1.96 in. Choi et al.^{10,11} developed a AMSLM with a pixel pitch of 7 μm . They developed a short channel oxide TFT as a switching device on a glass substrate.

In this paper, we will explain the bottleneck for a high-resolution AMSLM with an oxide TFT as a switching device and a liquid crystal as an optical modulator. And we will briefly describe the advantage and the challenge of using a phase-change material film as a new optical modulator.^{12,13}

2 High-Resolution Active Matrix Spatial Light Modulator on Glass Substrate

To create a large hologram image, it is indispensable to reconstruct hologram images through SLM with a large area.

Up to now, most of the SLM used for holography was made based on semiconductor technology. Semiconductor technology has the merits of high-performance Si MOSFET, ultrahigh-resolution patterning (tens of nm), and good operational stability. But the area of the fabricated device using semiconductor technology was limited to under 1-in.

*Address all correspondence to: Chi-Sun Hwang, E-mail: hwang-cs@etri.re.kr

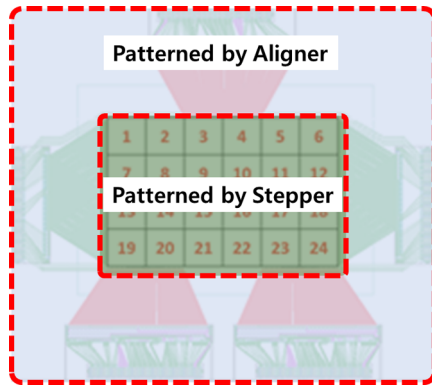


Fig. 1 Stitching process map for the combination of stepper and aligner tools. Active area composed of pixel array was patterned by stepper and the periphery area was patterned by aligner.

diagonal due to the finite field size of the photolithography tool.

LCoS and digital micromirror device (DMD) are the most widely used SLM devices in electronic holography. Owing to the complex driving circuits and high driving voltages, DMD devices have larger pixel pitch compared with LCoS. Considering the ease of reduction of pixel pitch and similarity to flat panel display technology, developing a reflective LCD display on glass substrate having a pixel pitch comparable with $1\ \mu\text{m}$ is determined as a final goal of our work.

2.1 Switching Device

Our approach to overcome the limitation of area in the SLM panel is to use display technology. Adoption of TFT-based backplane made on glass substrate will make it very easy to enlarge the panel area. But, to achieve ultrasmall pixel pitch (about $1\ \mu\text{m}$), it is indispensable to use photolithographic tools for semiconductor technology.

A stitching process was developed to make the SLM panel, the area of which was larger than the field size of the photolithographic tool. To reduce the process costs and time, the periphery area of the SLM panel was patterned using a projection aligner tool. Therefore, a special patterning process utilizing the combination of two different photolithographic tools was also developed as shown in Fig. 1.

In addition to the scale down of pattern size, the channel length and width of TFTs also should be reduced. It is generally known that, for the case of oxide semiconductor TFTs, the short channel effects do not appear up to very small channel length such as tens of nm. Therefore, oxide semiconductor TFTs can be good candidate for switching device of SLM panel. A short channel oxide TFT with channel length of $1\ \mu\text{m}$ was developed as shown in Fig. 2. For the case of the SLM on glass with $7\text{-}\mu\text{m}$ pixel pitch, oxide TFTs with $2\text{-}\mu\text{m}$ channel length was used.

Another merit of oxide semiconductor TFTs is extremely low off-currents. According to the scale down of pixel pitch, relative area of pixel capacitor compared with entire pixel area will be decreased. The allowable level of off-currents for switching TFTs in LCD should be lowered according to the decrease in the pixel pitch. Due to the wide band gap of the oxide semiconductor (larger than $3\ \text{eV}$), the off-currents of oxide semiconductor TFTs are fairly low compared with Si-based TFTs, such as a-Si TFTs and LTPS. Therefore,

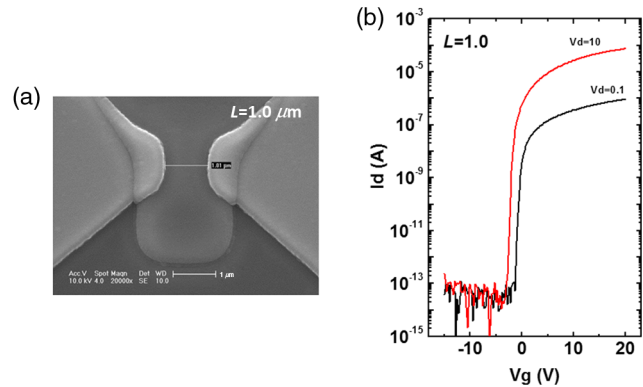


Fig. 2 Stitching short channel oxide TFT with channel length of $1\ \mu\text{m}$. (a) Top view, SEM image and (b) the transfer characteristics of $1\text{-}\mu\text{m}$ channel length of oxide TFT.

oxide semiconductor TFTs can cope with required off-current level of $1\text{-}\mu\text{m}$ pitch pixel.

To preserve the interference properties of reflected light, the optical flatness of the reflector should be maintained. An organic planarization layer was formed using coating and hard baking. Figure 3 shows the cross-section diagram of SLM on glass with the planarization layer, light block layer, and reflector layer.

2.2 Liquid Crystal

For an optical modulator, we used a liquid crystal and optimized it to our system with high anisotropic refractive index of $\Delta n = 0.25$ and minimum cell gap of $2.5\ \mu\text{m}$. It is well known that liquid crystal suffers a crosstalk among neighboring pixels when a pixel pitch approaches the cell gap distance.¹⁴ To verify the optical modulation characteristics when a pixel pitch is small, we designed the test pattern, such as Fig. 4. Pixel pitches are $1.6\ \mu\text{m}$ in the horizontal direction and $4.8\ \mu\text{m}$ in the vertical direction and every

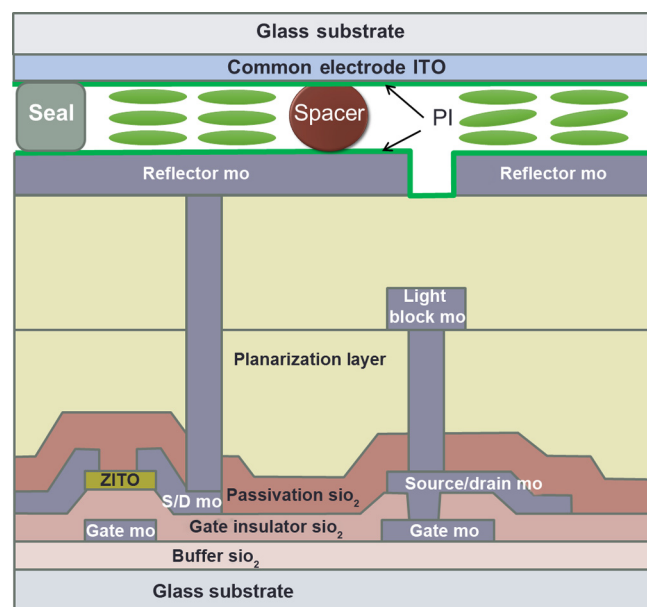


Fig. 3 Cross-section diagram of SLM on glass (SLMoG). ECB mode reflective LC cell is driven by oxide TFTs.

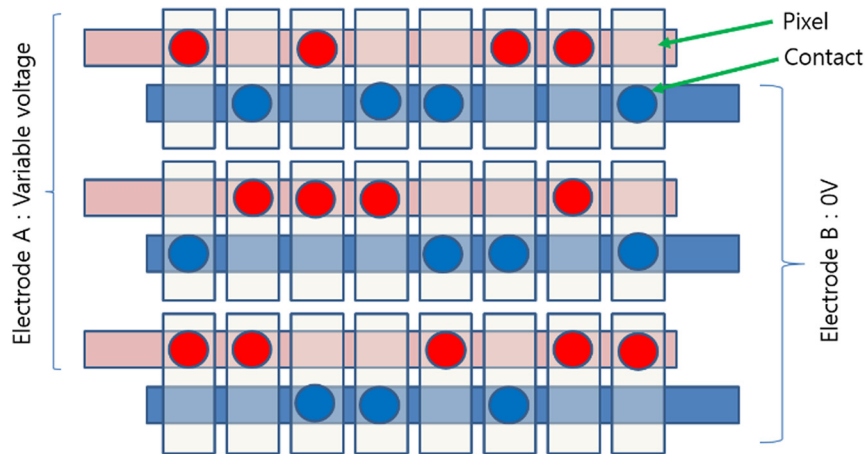


Fig. 4 Test pattern to verify the optical modulation characteristics. Pixel pitches are $1.6 \mu\text{m}$ in the horizontal direction and $4.8 \mu\text{m}$ in the vertical direction.

pixel is connected to the electrodes through contacts. The red contact is connected to the electrode A, which is used as a variable voltage source, whereas the blue contact is connected to the electrode B, which is connected to zero voltage. Therefore, when we apply the voltage to electrode A, liquid crystals on the pixels with red contacts will change their direction appropriate to the voltage while the liquid crystals on the pixels with blue contacts will not move.

The binary hologram is calculated as follows. The object is letters of “NANO SLM,” which are located 20 cm behind the SLM. The object’s light wave, which is propagated to the SLM plane, is calculated using the angular spectrum method.¹⁵ If the object wave’s amplitude is $|O(x, y)| \exp[j\varphi_{O(x,y)}]$ and the reference wave’s amplitude is $|R(x, y)| \exp[j\varphi_{R(x,y)}]$ at the SLM plane, then the binary hologram value for each pixel is designated as 1 when $\text{Re}[O(x, y)R^*(x, y)] = |O(x, y)| |R(x, y)| \cos[\varphi_{O(x,y)} - \varphi_{R(x,y)}] \geq 0$, otherwise it is zero. The pixels with the binary hologram value of 1 is connected to the variable voltage through red contact while those with the binary hologram value of zero are connected to constant zero voltage. Even though a liquid crystal works well according to the voltage, there are some concerns with respect to the observed reconstructed hologram image. When zero voltage is applied to the electrode A, we expect no hologram image because there will be no motion of a liquid crystal. However, the test pattern of Fig. 4 has the red and blue contact structures, which may induce some reconstructed hologram images.

Figure 5 shows a simple model for the contact structure of Fig. 4. When light shines on the contact structure of Fig. 5(a), there will be a diffracted beam from each contact. Red contacts are located exactly same to the pixel position of the binary hologram value of 1 so that the interference among diffraction lights from red contacts will reconstruct the hologram image, “NANO SLM,” at 20 cm distance from the SLM. Also, blue contacts are positioned at the complementary to the red contact position along the horizontal direction but shifted by d_{cont} along the vertical direction. Babinet’s principle¹ states that the electric field from the complementary points will have the same magnitude but 180 deg out of phase compared with that of the original points. Therefore, the diffracted lights from the blue contacts will make the same hologram, “NANO SLM,” with the same amplitude but 180 deg out of phase and shifted along the vertical direction by d_{cont} . Graphically, the diffracted electric field from the blue contacts in Fig. 5(a) can be considered as a summation of the diffracted electric fields from every blue contact in Fig. 5(b) and the diffracted electric fields from the green contacts in Fig. 5(c), which has the same amplitude but is 180 deg out of phase and shifted along the vertical direction by d_{cont} as compared with the diffracted electric field from the red contacts.

Figure 6 shows the phase difference, $\Delta\varphi$, at the reconstructed point between the diffracted electric fields from the red contacts and the green contacts. At horizontal plane where the zeroth-order hologram image along the vertical

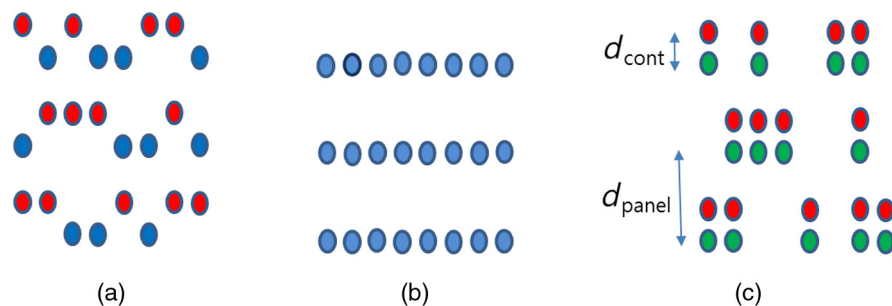


Fig. 5 Diffracted electric field from blue contacts of (a) can be considered as a summation of the diffracted electric field from every blue contact of (b) and the diffracted electric field from green contacts of (c), which has the same amplitude but 180 deg out of phase compared with that from the blue contacts.

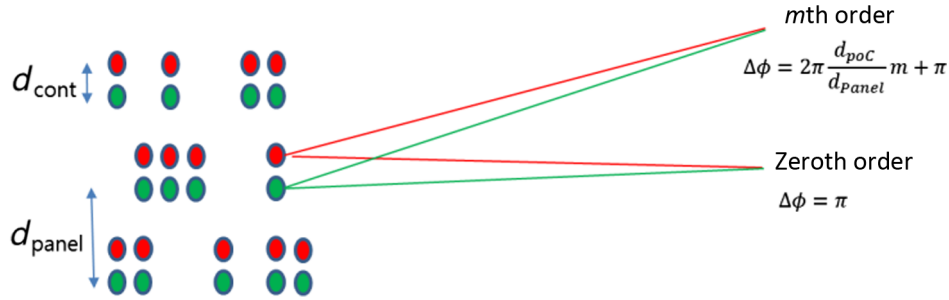


Fig. 6 Phase difference, $\Delta\phi$, at the reconstructed point between the diffracted electric field from the red contacts and that from the green contacts' hologram image estimation.

direction will appear, the phase difference, $\Delta\phi$, will be just π because there is no path difference from the contacts to the hologram reconstruction plane if we assume that the distance between the SLM and the reconstruction point is larger than the SLM size such that the electric field from the red contacts will interfere destructively with that from the green contacts, so that there will be no hologram due to the contact structure. The m 'th-order hologram image along the vertical direction occurs at the angle, $\sin \theta_m = m\lambda/d_{\text{panel}}$. Because there is a path difference between the red contacts and the green contacts to reconstruction point, $d_{\text{cont}} \sin \theta_m$, the phase difference, $\Delta\phi$, between the electric field from the red contacts and that from the green contacts will be as follows:

$$\Delta\phi = \pi + 2\pi m d_{\text{cont}} / d_{\text{panel}}. \quad (1)$$

Therefore, the phase difference depends on the ratio between the shifted contact distance and the panel pitch along the vertical direction, $d_{\text{cont}}/d_{\text{panel}}$. The reconstructed

hologram image will be bright due to the constructive interference when $\Delta\phi = 2k\pi$ but will disappear due to the destructive interference when $\Delta\phi = (2k - 1)\pi$, where k is the integer number.

Figure 7 shows the diffraction simulation result according to the variation of the shifted contact distance. The ratio between the shifted contact distance and the panel pitch along the vertical direction, $d_{\text{cont}}/d_{\text{panel}}$, is one-fifth for Figs. 7(a), 7(d), 7(g), and 7(j), two-fifths for Figs. 7(b), 7(e), 7(h), and 7(k), and three-fifths for Figs. 7(c), 7(f), 7(i), and 7(l), respectively. The zeroth-, first-, and second-order simulated hologram image along the vertical direction is Figs. 7(d)–7(f), 7(g)–7(i), 7(j), and 7(k), respectively. The simulation result shows that there is no zeroth-order hologram image along the vertical direction irrespective to the variation of the ratio between the shifted contact distance and the panel pitch along the vertical direction, $d_{\text{cont}}/d_{\text{panel}}$. In Figs. 7(d), 7(g), and 7(j), the ratio of $d_{\text{cont}}/d_{\text{panel}}$ is one-fifth, so that the phase difference of first- and second-order

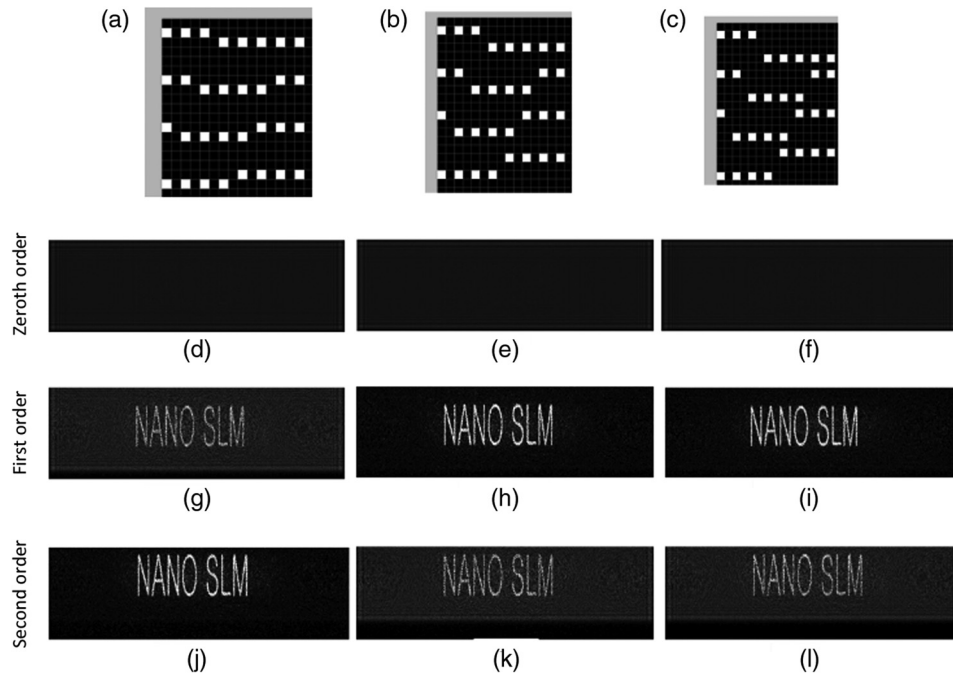


Fig. 7 Simulation results according to the variation of the shifted contact distance. The ratio between the shifted contact distance and the panel pitch along the vertical direction, $d_{\text{cont}}/d_{\text{panel}}$, is one-fifth for (a), (d), (g), (j), two-fifths for (b), (e), (h), (k), three-fifths for (c), (f), (i), (l) respectively. The zeroth-, first-, and second-order simulated hologram image along the vertical direction is shown in Figs. 7(d)–7(f), 7(g)–7(i), 7(j), and 7(k), respectively.

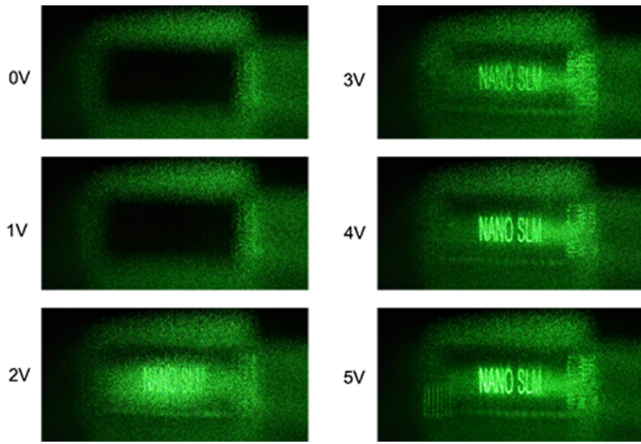


Fig. 8 Experimental results for hologram reconstruction with the variation of the applied voltage at the horizontal direction.

reconstructed hologram is $7\pi/5$ and $9\pi/5$, respectively, according to Eq. (1), so that second-order hologram image is brighter than that of the first-order hologram. In Figs. 7(b), 7(e), 7(h), and 7(k), the ratio of $d_{\text{cont}}/d_{\text{panel}}$ is two-fifths, so that the phase difference of first- and second-order reconstructed hologram between the electric field from the red contact and that from the green contact is $9\pi/5$ and $13\pi/5$, respectively, so that first-order hologram image is brighter than that of the second-order hologram. In Figs. 7(c), 7(f), 7(i), and 7(l), the ratio of $d_{\text{cont}}/d_{\text{panel}}$ is three-fifths, so that the phase difference of first- and second-order reconstructed hologram between the electric field from the red contact and that from the green contact is $11\pi/5$ and $17\pi/5$, respectively, so that first-order hologram image is brighter than that of the second-order hologram.

Figure 8 shows the experimental result for hologram reconstruction with the variation of the applied voltage at the horizontal direction. At zero voltage, there is no hologram image. When the applied voltage is 2 V, the faint hologram image starts to emerge. When the applied voltage is 4 V, the clear image with the maximum intensity is appeared. This voltage range is coinciding with the measured diffraction peak intensity with the applied voltage variation as shown in Fig. 9.

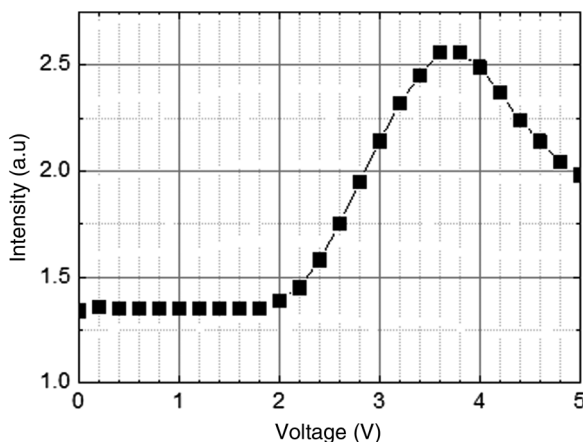


Fig. 9 Diffraction peak intensity as a function of voltage.

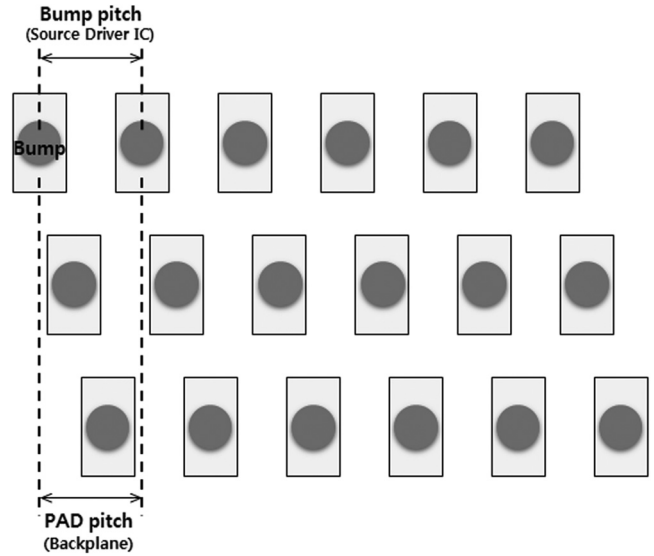


Fig. 10 Staggered-type bump configuration for small pitch bonding process.

2.3 Driving and Hologram Reconstruction

Driving a huge number of pixels is a gigantic task for the AMSLM. Owing to the short pixel pitch, the resolution of SLM will be very large compared with typical flat panel display.

Multiple numbers of scan driver chips and data driver chips should be bonded to the pad area of SLM. Therefore, to reduce the pad area, pad pitch should be reduced. The minimum pad pitch is limited by the diameter of conducting ball in anisotropic conductive film and align accuracy during bonding process. Multiple, staggered band pad structure is generally adopted for high-resolution display panel as shown in Fig. 10.

The number of channels for each driver chip should be increased to cope with high-resolution display, but the maximum number of channels is limited by the size of the driver chip. Considering the yield and price of the driver chip,

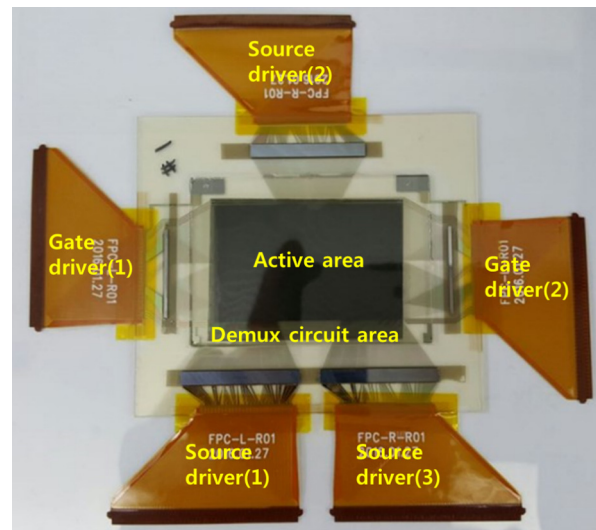


Fig. 11 Fabricated SLM on glass substrate. Three source drivers and two gate drivers were bonded for driving the SLM panel.

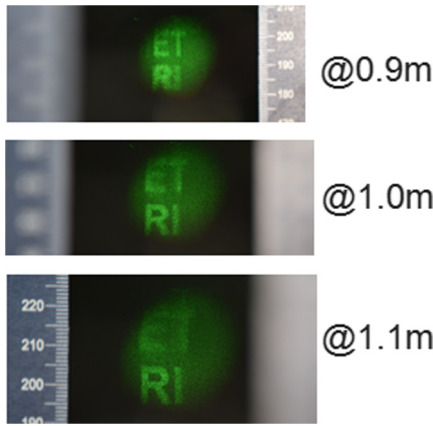


Fig. 12 Reconstructed hologram images by fabricated SLM on glass with 7- μ m pixel pitch.

the maximum size of the driver chip is limited by the field size of the photolithographic tool.

The allowed line time for each scan line is inversely proportional to the horizontal channel number of panel. An increase in the number of scan lines means the decrease in the line time. Therefore, for driving SLM, the current driving capability of switching TFTs should be enhanced. Data driving using a demux circuit can be used to deliver multiple signal at the cost of extra area for the demux circuit and complex driving signals.¹¹

We fabricated SLM on glass having 7- μ m pitch pixel driven by oxide TFTs. The size of SLM was 2 in. in diagonal.

The resolution of the SLM was 5.8 by 1.2 K and the SLM was driven by three source drivers and two gate drivers bonded on a glass panel as shown in Fig. 11.

Hologram images with depth were successfully reconstructed by SLM on the glass substrate as shown in Fig. 12. The “ET” was focused at 0.9 m and “RI” was focused at 1.1 m.

3 Phase Change Material as a Light Modulating Material

Ge₂Sb₂Te₅ (GST) is a phase change material, which induces a large change of refractive index about 1 when GST’s phase is transformed from an amorphous phase to a polycrystalline phase around 150°C as shown in Fig. 13. Due to the large optical contrast of GST film between two phases, many researchers have applied it to display devices,¹⁶ memory devices,¹⁷ and hologram devices.^{12,13} Lee et al.¹² used a thin resonant structure of metal/ITO (30 nm)/GST (7 nm)/ITO (20 nm) to enhance the diffraction efficiency by making the phase difference of π between an amorphous phase pixel and a polycrystalline phase pixel. Even though the physical thickness of the thin resonant structure is much below the wavelength of visible light, its structure works well for visible light and was successful to reconstruct striking hologram images.

One of the advantages using a resonant ITO/GST/ITO structure is to construct a color hologram image without a color filter. By changing the oxide layer thickness of metal/oxide/ITO (30 nm)/GST (7 nm)/ITO (20 nm), we can change the diffraction efficiency profile with a wavelength as

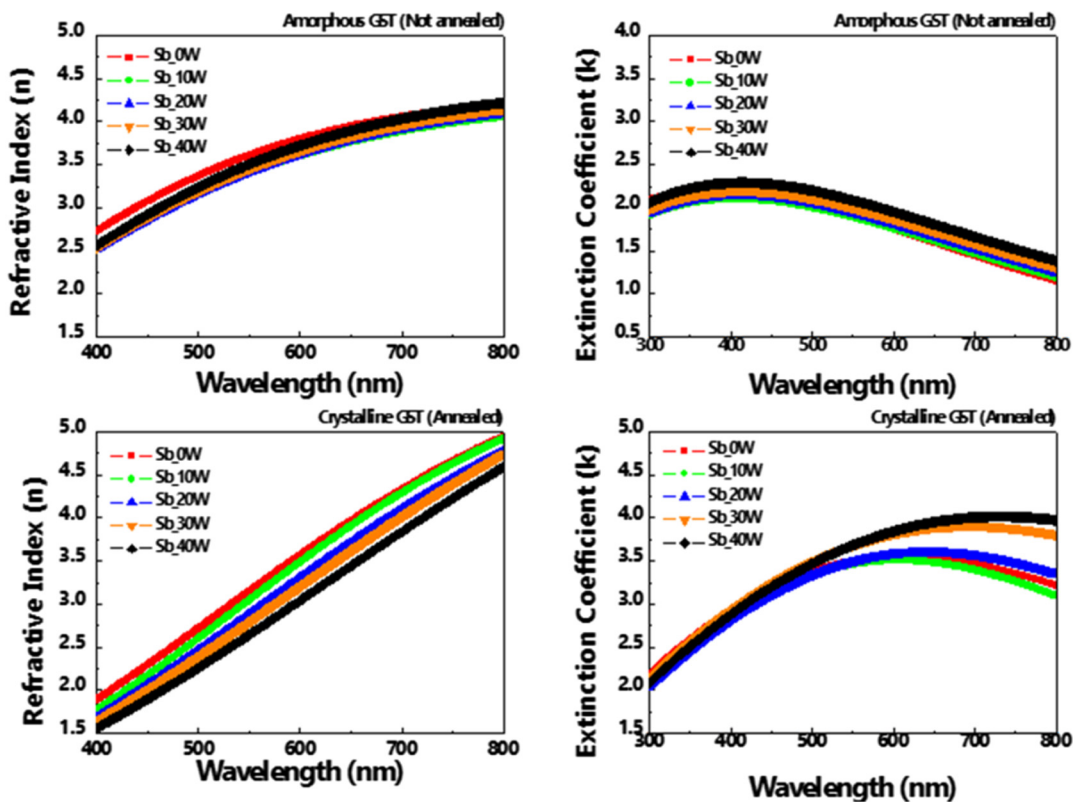


Fig. 13 Variation of reflective index and extinction coefficient of GST film according to the deposition power conditions for an antimony target.

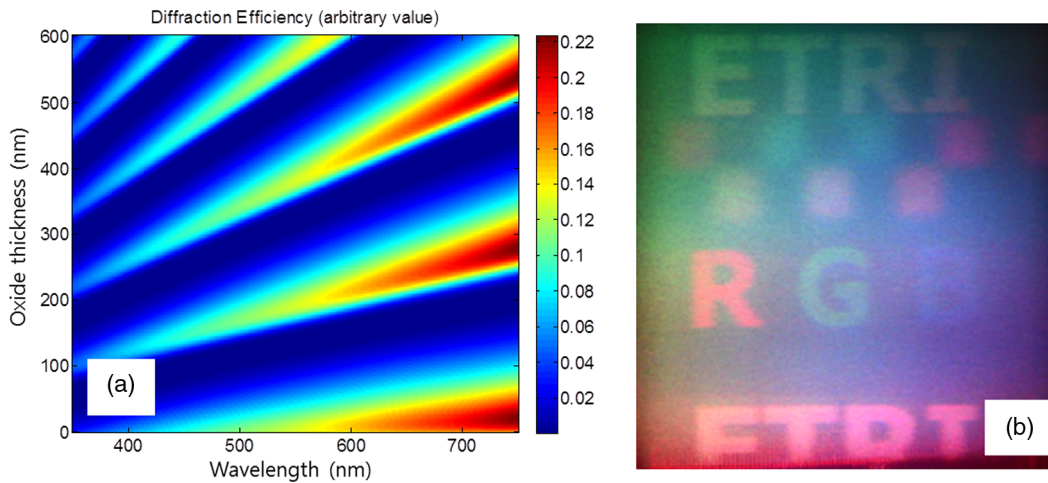


Fig. 14 (a) Diffraction efficiency variation with the underlying oxide thickness and (b) experimentally reconstructed color hologram image.

shown in Fig. 14(a). For the green wavelength of 532 nm, the optimum oxide thickness of the maximum diffraction efficiency appears at nearly 200, 400, and 600 nm. If we choose the oxide thickness of 200 nm, the diffraction efficiency for red wavelength is not negligible so that hologram images for green color will be interfered with red light resulting to yellow color. If we choose the oxide thickness of 600 nm, the diffraction efficiency for blue wavelength is not small, so the hologram image for green color will be interfered with blue light, resulting in a cyan color. Therefore, we choose the oxide thickness 400 nm for green, 300 nm for red, and 150 nm for blue. Figure 14(b) shows the reconstructed color hologram image using red, green, and blue laser. Each color image of R in red, G in green, and B in blue appears well and the combination color image of square also displayed correctly.

One of the challenges using a resonant ITO/GST/ITO structure is the stability issue. To transform GST film to an amorphous phase, we have to heat it above 600°C for

melting and quench it rapidly. During melting and quenching process, GST film suffers a large volume change and a structural change, which induce a void formation, such as Fig. 15. Although the thickness of the upper and lower ITO is the same to 20 and 30 nm, respectively, the thickness of the GST film is increased from 7 to 22 nm. The additional thickness comes from the agglomeration of the GST film and the void formation. The void formation is progressive as the number of hologram writing operation¹⁸ so that it limits the lifetime of resonant ITO/GST/ITO structure as AMSLM.

4 Summary

To integrate a switching device on the glass substrate, we designed a high-performance oxide thin-film transistor with a minimum channel length of 1 μm and a maximum processing temperature of 380°C. To drive a large number of data lines, we used multiple source drivers and data drivers as well.

For an optical modulator, we developed the test pattern and confirmed that a liquid crystal of a high anisotropic refractive index of 0.25 with a cell gap of 2.5 μm works well until pixel pitch is 1.6 μm . By optimizing the underlying oxide thickness of the resonant ITO/GST/ITO structure, we can show a color hologram without color filter.

Acknowledgments

This work was supported by “The Cross-Ministry Giga KOREA Project” grant funded by the Korea government (MSIT), (GK17D0100, Development of Telecommunications Terminal with Digital Holographic Table-top Display) and (GK17C0200, Development of Full 3-D Mobile Display Terminal and Its Contents).

References

1. E. Hecht, *Optics*, 2nd ed., Addison-Wesley, Reading, Massachusetts (1989).
2. Holotech, “3D digital hologram print,” 2016, <http://holotech3d.com>.
3. Y. Tsuchiyama and K. Matsushima, “Full-color large-scaled computer-generated holograms using RGB color filters,” *Opt. Express* **25**, 2016 (2017).
4. C. Williams et al., “Engineered pixels using active plasmonic holograms with liquid crystals,” *Phys. Status Solidi RRL* **9**, 125–129 (2015).
5. W. Wan, J. Gao, and X. Yang, “Full-color plasmonic metasurface holograms,” *ACS Nano* **10**, 10671–10680 (2016).

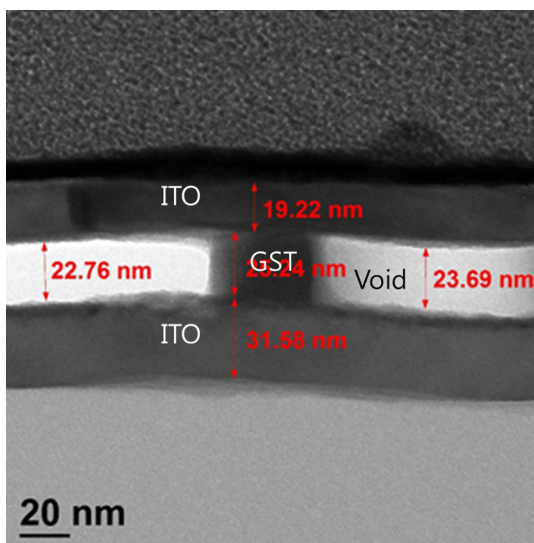


Fig. 15 TEM image of the failed ITO/GST/ITO film.

6. X. Li et al., "Multicolor 3D meta-holography by broadband plasmonic modulation," *Sci. Adv.* **2**, e1601102 (2016).
7. S. Malek, H. Ee, and R. Agarwa, "Strain multiplexed metasurface holograms on a stretchable substrate," *Nano Lett.* **17**, 3641–3645 (2017).
8. Holoeye, "Spatial light modulator," 2018, <http://holoeye.com/spatial-light-modulators/>.
9. H. S. Lee et al., "Holographic display and its applications," *SID 2017 Digest* **48**, 403–405 (2017).
10. J. H. Choi et al., "Toward sub-micron oxide thin-film transistors for digital holography," *SID 2017 Digest* **48**, 393–397 (2017).
11. J.-E. Pi et al., "Design of spatial light modulator on glass using oxide TFTs with lower off-state current," *SID 2017 Digest* **48**, 1178–1181 (2017).
12. S. Y. Lee et al., "Holographic image generation with a thin-film resonance caused by chalcogenide phase-change material," *Sci. Rep.* **7**, 41152 (2017).
13. S.Y. Lee et al., "Design method of tunable pixel with phase-change material for diffractive optical elements," *ETRI J.* **39**, 390–397 (2017).
14. D. Engstrom et al., "Calibration of spatial light modulators suffering from spatially varying phase response," *Opt. Express* **21**, 16086 (2013).
15. Y. H. Kim et al., "Non-uniform sampling and wide range angular spectrum method," *J. Opt.* **16**, 125710 (2014).
16. P. Hosseini, C. Wright, and H. Bhaskaran, "An optoelectronic framework enabled by low-dimensional phase-change films," *Nature* **511**, 206–211 (2014).
17. C. Ríos et al., "Integrated all-photonics non-volatile multi-level memory," *Nat. Photonics* **9**, 725–732 (2015).
18. K. Do et al., "TEM study on volume changes and void formation in Ge₂Sb₂Te₅ films, with repeated phase changes," *Electrochem. Solid State Lett.* **13**, H284 (2010).

Yong-Hae Kim is a principal researcher at Electronics and Telecommunications Research Institute (ETRI). He received his BS, MS, and PhD degrees in physics from Korea Advanced Institute of Science and Technology, Daejeon, Republic of Korea, in 1991, 1993, and 1997, respectively. He has been with the ETRI, Daejeon, Republic of Korea, since 2001, and his current research interests are spatial light modulators, 3-D display systems, and metamaterials.

Chi-Young Hwang received his BS degree in electrical engineering and his MS degree in electrical engineering and computer science from Seoul National University in 2010 and 2012, respectively. He joined the Electronics and Telecommunications Research Institute (ETRI) in 2012. His research interests include holography, nanophotonics, and metamaterials.

Ji Hun Choi received his BS and MS degrees in electrical engineering from Korea Advanced Institute of Science and Technology (KAIST), Daejeon, Republic of Korea, in 2012 and 2014, respectively. Since 2014, he has been with the Electronics and Telecommunications Research Institute (ETRI) as a member of research engineering staff. He worked on high-performance oxide transistors with high mobility based on double channel scheme. His current research interests include short channel oxide transistors and their application to high-resolution digital holography.

Jae-Eun Pi received his BS and MS degrees in electronics engineering from Konkuk University, Seoul, Republic of Korea, in 2009 and 2011, respectively. In 2011, he joined the oxide electronics research team of the Electronics and Telecommunications Research Institute (ETRI), Daejeon, Republic of Korea. Currently, he is working on reality display device research section as a senior researcher. His research interests include transparent flexible electronics and digital holography display.

Jong-Heon Yang received his BS degree in electrical engineering from Korea Advanced Institute of Science and Technology (KAIST), Korea, in 2000 and his MS degree in electronic engineering from Pohang University of Science and Technology (POSTECH), Pohang, Korea, in 2002. Currently, he is a senior engineering staff at the Electronics and Telecommunications Research Institute (ETRI), Daejeon, Korea.

Seong-M. Cho received his BS, MS, and PhD degrees in materials engineering from Pohang University of Science and Technology (POSTECH), Korea, in 1992, 1994, and 2001, respectively. From February 1994 to January 1996, he worked as a research engineer in the semiconductor division of Samsung Electronics. He has been with the Electronics and Telecommunications Research Institute (ETRI) as a principal researcher since 2001. His current research interests are electrochromic devices, holographic displays, and sensor devices.

Sang-Hoon Cheon received his BS, MS, and PhD degrees in electronics engineering and computer science from Korea Advanced Institute of Science and Technology (KAIST) in 1993, 1995, and 2001, respectively. In 2001, he joined Knowledge*on Inc. in Korea, where he was involved in 6 in. InGaP/GaAs HBT foundry service business. He worked on the large signal modeling for microwave devices during 2001 to 2003 and the development of power amplifier for WCDMA system during 2004 to 2005. In 2006, he moved to the Electronics and Telecommunications Research Institute (ETRI), Daejeon, Korea, where he has been involved in development on microbolometer for infrared focal plane arrays. His current research interests include wireless power transfer systems and digital holography.

Gi Heon Kim received his MS and PhD degrees in chemical engineering from Tokyo Institute of Technology, Japan, in 1996 and 2000, respectively. After his PhD course, he joined the Active Matrix (AM)-LCD Research Laboratory (2000–2001) at Samsung Electronics Inc., Korea. He specialized in the thermal-cured/photo-cured electronic materials for LCD displays. Currently, he is a principal member of Engineering Staff at the Electronics and Telecommunications Research Institute (ETRI), Daejeon, Korea from 2001, and works on transparent display technologies.

Kyunghee Choi received her BS degree from Kyungpook National University in 2004. She earned her MS degree in applied physics from Yonsei University in 2007 and then worked for Samsung Electronics till 2010. She achieved her PhD from Yonsei University in 2016. After PhD, she worked as a postdoctoral researcher at Yonsei University. Currently, she works at the Electronics and Telecommunications Research Institute as a senior researcher. Her research interests include oxide thin-film and van der Waals nanosheet-based electronics.

Chi-Sun Hwang received his BS degree from Seoul National University in 1991 and the PhD degree from KAIST in 1996, both in physics. From 1996 to 2000, he worked to make DRAM device at Hyundai Semiconductor Inc. Since 2000, he has joined the Electronics and Telecommunications Research Institute in Daejeon, Korea. His research focused on display technology based on AM FPD using TFTs, especially oxide TFTs. His recent interests are digital holography and novel switching devices.

Biographies for the other authors are not available.